

1 Benchmark data and software for assessing 2 genome-wide CRISPR-Cas9 screening pipelines

3 **Raffaele Iannuzzi^{1,†}, Ichcha Manipur^{2,†,‡}, Clare Pacini^{3,4}, Fiona M. Behan^{3,4,§}, Mario R.**
4 **Guarracino², Mathew J. Garnett^{3,4}, Aurora Savino^{1,*}, and Francesco Iorio^{1,3,4,*}**

5 ¹Human Technopole, Palazzo Italia, Viale Rita Levi Montalcini, 1 20157 Milan, Italy

6 ²Institute for High Performance Computing and Networking (ICAR), National Research Council, Via Pietro
7 Castellino, 111, 80131, Naples, Italy

8 ³Wellcome Sanger Institute, Wellcome Genome Campus, Hinxton, Cambridge, CB10 1SA, UK

9 ⁴Open Targets, Wellcome Genome Campus, Hinxton, Cambridge, CB10 1SA, UK

10 ^{*}corresponding author(s): Aurora Savino (aurora.savino@fht.org) and Francesco Iorio (francesco.iorio@fht.org)

11 [†]these authors contributed equally to this work

12 [‡]Current address: Cambridge Institute of Therapeutic Immunology & Infectious Disease, University of Cambridge,
13 UK

14 [§]Current address: GSK Medicines Research Centre, Gunnels Wood Road, Stevenage, Hertfordshire, SG1 2NY,
15 United Kingdom

16 ABSTRACT

17 Genome-wide recessive genetic screens using lentiviral CRISPR-guide RNA libraries are widely performed in mammalian cells to functionally characterise individual genes and for the discovery of new anti-cancer therapeutic targets. As the effectiveness of such powerful and precise tools for cancer pharmacogenomic is emerging, reference datasets for their quality assessment and the validation of the underlying experimental pipelines are becoming increasingly necessary. Here, we provide a dataset, an R package, and metrics for the assessment of novel experimental pipelines upon the execution of a single calibration viability screen of the HT-29 human colon cancer cell line, employing a commercially available genome-wide library of single guide RNAs: the Human Improved Genome-wide Knockout CRISPR (Sanger) Library. This dataset contains results from screening the HT-29 in multiple batches with the Sanger library, and outcomes from several levels of quality control tests on the resulting data. Data and accompanying R package can be used as a toolkit for benchmarking newly established experimental pipelines for CRISPR-Cas9 recessive screens, via the generation of a final quality-control report.

18 Background & Summary

19 Genome-wide CRISPR-Cas9 screens are being increasingly employed to explore various genotype–phenotype associations¹,
20 to identify genes whose function is essential for cell viability and proliferation (essential genes or fitness genes), and new
21 potential targets for personalised anti-cancer therapies^{2–7}. Several methods exist for assessing the quality of the datasets
22 derived from these screens, evaluating sequence quality, single-guide RNA (sgRNA) count distributions and negatively selected
23 genes⁸. In addition, comprehensive analyses have been performed to evaluate the level of reproducibility and integrability of
24 large-scale cancer dependency datasets assembled from independently performed CRISPR-Cas9 screens^{9,10}. However, to date
25 no easy-to-use toolkit is available to assist experimental scientists in validating newly established experimental pipelines for
26 genome-wide CRISPR-Cas9 genetic screens using pooled sgRNA libraries.

27 In Behan *et al.*⁷, we performed genome-wide CRISPR–Cas9 fitness screens of 339 cancer cell lines from the Cell Models
28 Passport panel¹¹. We analysed the data resulting from this screen with an ad-hoc computational pipeline designed to identify
29 new anti-cancer therapeutic targets at a genome-scale. To this aim, we defined quality control assessment practices and applied
30 stringent quality control criteria, finally retaining data for 324 cell lines. Via a target-prioritisation bioinformatics pipeline we
31 predicted and validated a novel selective therapeutic target for cancers with microsatellite instability: the Werner syndrome
32 ATP-dependent helicase⁷ (a finding simultaneously reported by other independent studies^{12–14}). Results and datasets from this
33 study are available for download on the Project Score data portal (<https://score.depmap.sanger.ac.uk/>). As part
34 of this effort, we screened the HT-29 colorectal cancer cell line with the same experimental settings in multiple batches and
35 dates, to assess robustness and reproducibility of our experimental pipeline.

36
37 Here, we provide high-quality data from 30 screens of the HT-29 cell line yielding reliable gene essentiality profiles, and a

38 dedicated analytical tool implemented into an R package¹⁵. We propose the use of this data and software as a simple toolkit to
39 benchmark and validate newly established genome-scale CRISPR-Cas9 knock-out screening pipelines employing the Human
40 Improved Genome-wide Knockout CRISPR sgRNA library (the Sanger library, available on Addgene)¹⁶. By performing a
41 single calibration screen of the HT-29 cell line with the Sanger library and settings described in Behan *et al.*⁷, experimental
42 scientists can assess quality and reproducibility of their pipeline by processing resulting data with our R package, which
43 implements a diversified set of metrics to compare new data with expected outcomes.
44 Data and code, including the *HT29benchmark* R package, are available at <https://score.depmap.sanger.ac.uk/downloads>, FigShare¹⁷ and <https://iorio-apps.fht.org/>.
45

46 Methods

47 Reference dataset generation: CRISPR-Cas9 screens

48 The protocol used for the generation of Cas9-expressing HT-29 cell lines and transduction of the Sanger library¹⁶ is described
49 in Behan *et al.*⁷. Briefly, we employed the commercially available Sanger Library v1.0 (Addgene, 67989), encompassing
50 90,709 sgRNAs targeting 18,009 genes, and a second version of the same library (Sanger library v1.1) including all the
51 sgRNAs from v1.0 plus 1,004 non-targeting sgRNAs, and 5 additional sgRNAs targeting 1,876 selected genes encoding kinases,
52 epigenetics-related proteins and pre-defined fitness genes, for a total of 10,381 additional sgRNAs. Cells were grown for
53 14 days following transduction with the Sanger Library (v1.0 or v1.1) and selection, and then collected for DNA extraction.
54 Illumina sequencing and sgRNA counting were performed as described in Tzelepis *et al.*¹⁶. Experiment identifiers and settings
55 are fully described in Supplementary Table 1, summarised in Table 1 and further detailed in the Extended data Fig. 2j of Behan
56 *et al.*⁷.

57 Overall, we performed 2 independent experiments with the Sanger v1.0 library and 4 experiments with the Sanger v1.1 library.
58 These can be regarded as biological replicates of HT-29 CRISPR screens, while each experiment has been performed with a
59 varying number of technical replicates (from 3 to 9) for a total of 30 individual screens, as indicated in Table 1.

60 Reference dataset preprocessing

61 We quantified and pre-processed post library-transduction and control library-plasmid sgRNA read counts as described in
62 Behan *et al.*⁷, removing sgRNAs with less than 30 reads in the library-plasmid and keeping only sgRNAs in common between
63 the two versions of the Sanger libraries. Subsequently, we normalised counts across replicates, scaling each sample by total
64 number of reads. Post normalisation, we computed sgRNA log fold-changes () between individual replicate read counts and
65 library-plasmid read counts for each experiment, keeping the replicates separated (Supplementary Fig. 1). These pre-processing
66 steps were performed with the *CCR.NormfoldChanges* function of our previously published *CRISPRcleanR* R package¹⁸,
67 using default parameters. Resulting data at all intermediate pre-processing levels are included in our reference dataset (available
68 at: <https://score.depmap.sanger.ac.uk/downloads> and on FigShare¹⁷).

69 Example of user provided data

70 In order to demonstrate and test the diverse functionalities of the *HT29benchmarkR* package, we used (as an example of
71 user-provided data) a lower quality screen of the HT-29 cell line, which was discarded from the analysis set in Behan *et al.*⁷, and
72 encompasses six technical replicates of an HT-29 screen, obtained following the same screening protocol and the pre-processing
73 steps described above.

74 Receiver operating characteristic analysis

75 To compute receiver operating characteristic (ROC) and precision/recall (PrRc) curves, required to perform high-level quality
76 control assessment of CRISPR-cas9 screens, we used the *HT29R.individualROC* function of the *HT29benchmarkR*
77 package, which implements the *ROC_Curve* and *PrRc_Curve* functions of the *CRISPRcleanR* package¹⁸ (version 2.2.1),
78 which itself implements the *roc* and *coords* functions of the *pROC* open-source R package (version 1.18.0)¹⁹.

79 Fitness-effect threshold

80 Following the approach we presented in Pacini *et al.*¹⁰, we employed a rank-based method to compute a fitness effect
81 significance threshold for each HT-29 reference screen, thus identifying a set of significantly depleted (or essential) genes at a
82 fixed level of 5% false discovery rate (FDR), based on their depletion log fold-changes (LFCs). Specifically, in a given screen,
83 we first ranked all genes in increasing order of average depletion LFCs (based on the differential abundance of their targeting
84 sgRNAs at the end of the assay versus plasmid control). Then we scrolled the obtained ranked list from the most depleted gene
85 to the least depleted one, and we considered the depletion LFC *r* of each encountered gene as a potential threshold, i.e. calling
86 all genes with a depletion log fold-change $< r$ significantly depleted.

87 Among the significantly depleted genes at a candidate threshold *r* we focused only on those belonging to any of two prior

88 known sets of essential (E) and non-essential (N) genes². Considering these two sets as reference positive and negative
89 controls, respectively, allowed us to compute a positive predictive value (PPV), thus a false discovery rate (FDR = 1 –
90 PPV). We finally select as fitness-effect significance threshold the largest r , yielding an FDR ≤ 0.05 . We implemented this
91 procedure using the `roc` and `coords` functions of the *pROC* open-source R package (version 1.18.0)¹⁹ implemented in the
92 `HT29R.ROCanalysis` and `HT29R.FDRconsensus` functions of the *HT29benchmark* R package.

93 Data visualisation

94 For data visualisation, we used R base graphics plus the following R libraries and packages (listed in alphabetical order), all
95 available on bioconductor²⁰ or on The Comprehensive R Archive Network (CRAN) repository: *crayon* version 1.5.1; *enrichPlot*
96 version 1.14.2; *GGally* version 2.1.2; *ggplot2* version 3.3.6; *ggrastr* version 1.0.1; *grid* version 4.1.0; *gridExtra* version 2.3;
97 *gttable* version 0.3.0; *RcolorBrewer* version 1.1.3; *VennDiagram* version 1.7.3; *vioplot* version 0.3.7²¹.

98 Enrichment analysis

99 We performed Gene Ontology (GO) enrichment analysis to identify biological processes over-represented in the list of HT-29-
100 specific fitness genes. For this analysis, we used the *org.Hs.eg.db* R package (version 3.14.0) to retrieve the gene universe and
101 the *clusterProfiler* R package (version 4.2.2) to perform the enrichment analysis of the HT-29-specific genes.

102 Data Records

103 The entire HT-29 reference dataset described here is available at different intermediate levels of pre-processing on the Project
104 Score website <https://score.depmap.sanger.ac.uk/downloads> and on FigShare¹⁷ (https://figshare.com/articles/dataset/HT29_reference_dataset/20480544).

105 The main data folder contains four subfolders:

- 107 • **00_rawCounts_assembled** - Containing one tsv file for each HT-29 screen. Each file comprises the control library-plasmid
108 sgRNA counts, as well as 14 days post-selection sgRNA counts across technical replicates;
- 109 • **01_normalised_and_FCs** - Containing Rdata files of normalised counts and depletion Log fold-changes (LFCs) for the
110 six screens, plots of counts' distribution pre- and post-normalisation, and boxplots showing LFCs' distributions (PDF
111 files);
- 112 • **02_lowLev_QC** - subdivided in the following four subfolders:
 - 113 1. FC_distr - log fold-change distribution plots for each of the six screens, in PDF;
 - 114 2. FC_Rep_corr - Between-replicates correlation plots for each of the six screens, in PDF;
 - 115 3. PrRc_curves_ind_rep - Plots of replicate Precision Recall (PrRc) curves quantifying essential/non-essential genes'
116 classification performances across the six screens, in PDF;
 - 117 4. ROC_curves_ind_rep - Plots of replicate Receiver Operating Characteristic (ROC) curves quantifying essential/non-
118 essential genes' classification performances across the six screens, in PDF;
- 119 • **03_HL_QC_Stats** - Density plots of depletion LFCs for reference gene sets across the six experiments with quality
120 control values, in PDF.

121 Technical validation

122 In the *HT29benchmark* package we have implemented a set of reference metrics for the assessment of quality and reproducibility
123 of CRISPR screens. In particular, these metrics assess sgRNA LFC distributions, screen outcomes' reproducibility across
124 technical replicates, inter-screen similarity, and screens' ability to detect known fitness genes among the depleted ones. Here,
125 we report results from applying these metrics to technically validate our HT-29 reference dataset, as well as to showcase how
126 our package can be used to evaluate an example of user-provided dataset. Furthermore, we report a set of reliable HT-29 specific
127 fitness genes, which we have identified via a joint analysis of all the screens in our reference dataset. These genes are expected
128 to be detected as significantly essential in any CRISPR screen of the HT-29 cell line performed with the experimental settings
129 underlying the generation of our reference dataset⁷, and using the Sanger library¹⁶. All the technical validations presented here
130 can be re-executed by a user on its own data through our *HT29benchmarkR* package.

131 **HT29benchmarkR package overview**

132 The *HT29benchmarkR* package allows assessing quality and reproducibility of both reference and user-provided CRISPR
133 screens of the HT-29 cell lines employing the Sanger library and the experimental settings described in Behan *et al.*⁷. More
134 in detail, the *HT29benchmark* package implements several routines from our previously published *CRISPRcleanR* package¹⁸
135 wrapped in novel ad-hoc designed functions, providing a powerful and easy-to-use tool able to:

- 136 • Download the HT-29 reference dataset;
- 137 • Inspect and visualise sgRNAs depletion LFC distributions of each screen;
- 138 • Evaluate intra-screen reproducibility of depletion LFCs at the sgRNA level, as well as at the gene level;
- 139 • Evaluate inter-screen similarity of depletion LFCs at the sgRNA level, as well as at the gene-level;
- 140 • Evaluate individual screen performances in correctly partitioning known essential (positive control) and known non-
141 essential (negative control) genes, when considered as rank based classifiers based on gene depletion LFCs - through
142 ROC and PrRc curves, as well as Recall at a fixed False Discovery Rate (FDR);
- 143 • Visualise depletion LFC distributions for positive and negative control genes (as well as for their targeting sgRNAs) and
144 compute Glass's Δ scores quantifying the difference of their average depletion LFCs in the screen under consideration;
- 145 • Derive HT-29-specific essential/non-essential genes, by analysing all screens in the reference dataset jointly and then to
146 use these sets as positive/negative controls to estimate to what extent a user-provided screen meets expectations, based on
147 the metrics listed above.

148 **Inspection of sgRNA log fold-change distributions**

149 The *HT29R.FCDistributions* function of the *HT29benchmark* package allows inspecting sgRNA LFC distributions and
150 it computes statistics such as average range, median, interquartile range, 10th – 90th percentile range, skewness and kurtosis.
151 We have applied these metrics to the screens in our reference HT-29 dataset, observing that the LFC distributions and their
152 parameters meet expected shape/values of a typical CRISPR-Cas9 recessive screen^{22,23} (Fig. 1a).
153 This function can also take in input a user-provided screen, allowing a comparison between reference and new data, which
154 might unveil unexpected distribution shapes, outliers and other data inconsistencies, thus allowing a first exploratory assessment
155 of a new screen (Fig. 1a).

156 **Intra-screen reproducibility assessment**

157 To assess screen replicates' reproducibility, we defined a reliable measure of intra-screen similarity. In our previous work⁷, we
158 observed that comparing replicates of the same screen at the level of absolute post-transduction sgRNA count profiles produces
159 meaningless outcomes, due to individual sgRNA counts varying in different ranges, which are determined by their initial amount
160 in the library-plasmid. This produces a strong Yule-Simpson effect²⁴ resulting in a generally high background correlation
161 between any pair of genome-wide sgRNA count profiles. As a result, when using this criterion as a reproducibility metric, pairs
162 of replicates of the same screen are indistinguishable from two individual replicates of different screens (Supplementary Fig.
163 2a).

164 Due to only a small fraction of genes having an impact on cellular fitness upon CRISPR-Cas9 targeting, pairs of replicates from
165 different screens tend to yield generally highly correlated dependency profiles even when considering sgRNA (or gene level)
166 depletion LFCs (Supplementary Fig. 2bc) instead of absolute counts.

167 For these reasons, in Behan *et al.*⁷ we followed an approach similar to that introduced in Ballouz *et al.*²⁵ and identified a set
168 of library-specific informative, and highly reproducible, sgRNAs pairs targeting the same gene and with an average pairwise
169 correlation of their depletion LFC pattern greater than 0.6 across a set of 332 cell lines from Project Score⁷. This yielded a
170 total of 838 unique informative sgRNAs. Per construction, the depletion patterns of these sgRNAs are both reproducible and
171 informative, as they involve genes carrying an actual and sufficiently variable fitness signal.

172 When considering these informative sgRNAs only, correlation scores from comparing replicates of the same screens were
173 significantly higher than those from comparing pairs of replicates from different screens (Supplementary Fig. 2de) of the
174 Project Score dataset. This allowed us to define a threshold value discriminating the two distributions both at sgRNA- and
175 gene-level ($R = 0.55$ and $R = 0.68$, respectively), as defined in Behan *et al.*⁷ (Fig. 1bc), and to use this value as a required
176 minimal quality while evaluating intra-screen reproducibility.

177 The function *HT29R.evaluateReps* of the *HT29benchmark* package allows a robust assessment of input screens, producing
178 plots like those shown in Fig. 1bc. All technical replicate pairs in the HT-29 reference screens exceed the reproducibility
179 threshold defined in Behan *et al.*⁷ (blue circles in Fig. 1bc). Moreover, inter-screen reproducibility of user-provided data can

180 also be evaluated (magenta circles in Fig. 1bc), and results visualised and compared with those observed for the reference
181 HT-29 dataset.

182 **Inter-screen similarity evaluation**

183 As a second measure of reproducibility, we evaluated results' comparability across different screens. Thus, we considered
184 genes (or sgRNAs) passing pre-processing filters in all the six HT-29 screens, computed LFCs' profiles and averaged them
185 across technical replicates, ending up with six different LFC profiles (one for each screen). We computed Pearson's cor-
186 relation scores comparing each pair of these profiles. This analysis is performed (and results can be visualised) by the
187 `HT29R.expSimilarity` function included in our `HT29benchmark` package, which (as before) can be also used on a user-
188 provided screen to assess its similarity, in terms of depletion LFCs, to the six HT-29 reference screens. For consistency with the
189 reproducibility measure introduced in the previous section, this function allows considering the entire Sanger library or highly
190 informative sgRNAs only, and to evaluate screens' similarity both at the sgRNA and gene level (Fig. 2 and Supplementary Fig.
191 3abc).

192 **Screens classification performances**

193 The ability to discriminate prior known essential and non-essential genes based on their depletion LFC observed in a CRISPR-
194 Cas9 recessive screen is widely used to assess the quality of that screen^{3,5,7,9,10,23,26,27}.

195 In particular, a good quality CRISPR screen will tend to detect genes involved in fundamental cellular processes, and other *core*
196 *fitness genes*, as highly depleted invariantly across screened cell types. Robust reference sets of core essential and non-essential
197 genes can be used as a gold standard to evaluate screens' performances^{26,28}. The `HT29R.PhenoIntensity` function
198 provides a measure of screen quality by leveraging the intensity of the phenotype exerted by inactivating these genes. To
199 quantify this effect, in Behan *et al.*⁷ we computed Glass's Δ score²⁹ computed respectively for reference essential genes (i.e.,
200 genes that reduce cellular viability/fitness upon inactivation³) (E) and (more stringently) for ribosomal protein genes³⁰ (R)
201 genes. These scores account for the difference between the average depletion LFCs of the genes in E (respectively R) and
202 that of genes known to be non-essential³ (N) in relation to the standard deviation of the depletion LFCs of the genes in E
203 (respectively R), as it follows:

$$\Delta(X) = |\mu[\text{LFC}(x \in X)] - \mu[\text{LFC}(x \in N)]| / \sigma[\text{LFC}(x \in X)],$$

204 where $X \in E, R$, and μ and σ indicate mean and standard deviation, respectively. The Δ s for the screens in the reference dataset
205 were consistently > 2 for ribosomal protein genes and > 1 for the other essential genes (with a Glass's *Delta* > 0.8 widely
206 considered an indicator of large effect size), thus indicative of generally good data quality (Fig. 3a and Supplementary Fig. 4).
207 In addition, as depicted in Fig. 3ab, in this case applying this metric to the example user-provided screen yielded values within
208 the expected ranges.

209 In addition to the Glass's Δ s, we implemented and included in our package the `HT29R.ROCanalysis` function com-
210 puting and visualising ROC and PrRc curves to evaluate the ability of each screen in correctly partitioning prior known
211 essential (E) and non-essential (N) genes, when considered as a rank based classifier based on sgRNA- or gene-depletion-
212 LFCs (as explained in the previous sections). Applying this function to the HT-29 reference dataset, as well as to example
213 user-provided data, yielded the results shown in Fig. 3cd. Also in this case our reference dataset yielded very good quality scores.

214 Finally, as a further quality assessment and reference to the user, we computed fitness effect significance thresholds
215 employing prior known essential and non-essential genes³¹ at different FDR levels, and we quantified corresponding Recall
216 values of prior known essential-genes, as well as a novel set of human core-fitness genes introduced in Behan *et al.*⁷ and various
217 sets of other essential genes (all available in the `CRISPRcleanR` package¹⁸ (Supplementary Fig. 5 and Supplementary Table 2)).
218 Also these results confirmed the high quality of our reference dataset.

219 **HT-29-specific fitness genes**

220 We assembled a list of genes that are consensually significantly depleted across all our reference HT-29 screens, thus should be
221 observed as significantly depleted in new screens of the HT-29 cell line performed with the Sanger library¹⁶ and the experimental
222 setting described in Behan *et al.*⁷. First of all, for each reference HT-29 screen we identified a set of genes significantly
223 depleted at a 5% FDR and its complement, i.e. a set of genes not significantly depleted, using reference sets of essential
224 (E) and non-essential (N) genes³¹ to compute significance thresholds, as explained in the previous sections. Intersecting all
225 these sets of screen-specific significantly depleted, respectively non depleted, genes yielded a high-confidence set of HT-29
226 specific essential, respectively non-essential, genes. We assessed how each reference screen discriminated these two sets in
227 228

229 terms of Glass's Δ^{29} or Cohen's d^{32} , computed as explained in the previous sections. This allowed us to define again a set of
230 expected values to evaluate a newly performed screen of the HT-29 (Fig 4abc). These HT-29-specific fitness genes are also
231 provided in Supplementary Table 3, partitioned into three tiers based on their average depletion LFCs across screens. These
232 genes showed a fairly consistent depletion LFCs across screens (Fig 4d) and were significantly enriched for previously report
233 human essential genes (Fisher's exact test $p = 7.1 * 10 - 221$, Fig. 4c) and for fundamental biological processes (BP) such as
234 "ribosome biogenesis" and "RNA splicing" (Fig. 4e), confirming their reliability.

235 **Usage Notes**

236 The HT-29 reference dataset can be manually downloaded at <https://score.depmap.sanger.ac.uk/downloads>
237 or <http://iorio-apps.fht.org/>, or on FigShare¹⁷. Alternatively, the function HT29R.download_ref_dataset
238 of the HT29benchmark package can be used to download the reference dataset within an R session. A vignette with instructions
239 on how to perform a quality assessment of a newly performed screen of the HT-29 cell line employing Sanger library¹⁶ and
240 settings described in Behan *et al.*⁷ is provided with the package, together with a wrap-function that performs all the assessment
241 steps and produces a final report in PDF format, as well as reproducing all the figures we presented here.

242
243 Users have a non-exclusive, non-transferable right to use data files for internal proprietary research and educational purposes,
244 including target, biomarker and drug discovery. Excluded from this licence are the use of the data (in whole or any significant
245 part) for resale either alone or in combination with additional data/product offerings, or for provision of commercial services.
246 Both package and reference data are experimental and academic in nature and are not licensed or certified by any regulatory
247 body. Furthermore, data access is provided on an "as is" basis and excludes all warranties of any kind (express or implied).

248 **Code availability**

249 The R code used for generating this dataset, for its QC assessment, as well as to evaluate the quality of a user-provided screen and
250 to reproduce all the figures presented here is available at <https://github.com/francescojm/HT29benchmark>.

251 **References**

- 252 1. Koike-Yusa, H., Li, Y., Tan, E.-P., Velasco-Herrera, M. D. C. & Yusa, K. Genome-wide recessive genetic screening in
253 mammalian cells with a lentiviral CRISPR-guide RNA library. *Nat. Biotechnol.* **32**, 267–273 (2014).
- 254 2. Hart, T. *et al.* Evaluation and design of Genome-Wide CRISPR/SpCas9 knockout screens. *G3* **7**, 2719–2727 (2017).
- 255 3. Hart, T. *et al.* High-Resolution CRISPR Screens Reveal Fitness Genes and Genotype-Specific Cancer Liabilities. *Cell* **163**,
256 1515–1526 (2015).
- 257 4. Shalem, O. *et al.* Genome-scale CRISPR-Cas9 knockout screening in human cells. *Science* **343**, 84–87 (2014).
- 258 5. Meyers, R. M. *et al.* Computational correction of copy number effect improves specificity of CRISPR–Cas9 essentiality
259 screens in cancer cells. *Nat. Genet.* **49**, 1779–1784 (2017).
- 260 6. Wang, T. *et al.* Identification and characterization of essential genes in the human genome. *Science* **350**, 1096–1101 (2015).
- 261 7. Behan, F. M. *et al.* Prioritization of cancer therapeutic targets using CRISPR-Cas9 screens. *Nature* **568**, 511–516 (2019).
- 262 8. Li, W. *et al.* Quality control, modeling, and visualization of CRISPR screens with MAGeCK-VISPR. *Genome Biol.* **16**,
263 281 (2015).
- 264 9. Dempster, J. *et al.* Agreement between two large pan-cancer genome-scale CRISPR knock-out datasets. *Nat. Commun.* **10**,
265 5817 (2019).
- 266 10. Pacini, C. *et al.* Integrated cross-study datasets of genetic dependencies in cancer. *Nat. Commun.* **12**, 1661 (2021).
- 267 11. van der Meer, D. *et al.* Cell model passports—a hub for clinical, genetic and functional datasets of preclinical cancer
268 models. *Nucleic Acids Res.* **47**, D923–D929 (2019).
- 269 12. Chan, E. M. *et al.* WRN helicase is a synthetic lethal target in microsatellite unstable cancers. *Nature* **568**, 551–556 (2019).
- 270 13. Lieb, S. *et al.* Werner syndrome helicase is a selective vulnerability of microsatellite instability-high tumor cells. *Elife* **8**
271 (2019).
- 272 14. Kategaya, L., Perumal, S. K., Hager, J. H. & Belmont, L. D. Werner syndrome helicase is required for the survival of
273 cancer cells with microsatellite instability. *iScience* **13**, 488–497 (2019).

274 15. R Core Team. *R: A Language and Environment for Statistical Computing*. R Foundation for Statistical Computing, Vienna,
275 Austria (2016).

276 16. Tzelepis, K. *et al.* A CRISPR Dropout Screen Identifies Genetic Vulnerabilities and Therapeutic Targets in Acute Myeloid
277 Leukemia. *Cell Rep.* **17**, 1193–1205 (2016).

278 17. Behan, M., Iorio, F. & Garnett, J., G. HT29 reference dataset. figshare. dataset.
279 <https://doi.org/10.6084/m9.figshare.20480544> (2022).

280 18. Iorio, F. *et al.* Unsupervised correction of gene-independent cell responses to CRISPR-Cas9 targeting. *BMC Genomics* **19**,
281 604 (2018).

282 19. Robin, X. *et al.* pROC: an open-source package for R and S+ to analyze and compare ROC curves. *BMC Bioinforma.* **12**,
283 77 (2011).

284 20. Gentleman, R. C. *et al.* Bioconductor: open software development for computational biology and bioinformatics. *Genome
Biol.* **5**, R80 (2004).

286 21. Chen, H. & Boutros, P. C. VennDiagram: a package for the generation of highly-customizable venn and euler diagrams in
287 R. *BMC Bioinforma.* **12**, 35 (2011).

288 22. Bock, C. *et al.* High-content CRISPR screening. *Nat. Rev. Methods Primers* **2**, 1–23 (2022).

289 23. Hanna, R. E. & Doench, J. G. Design and analysis of CRISPR–Cas experiments. *Nat. Biotechnol.* **38**, 813–823 (2020).

290 24. Wagner, C. H. Simpson’s paradox in real life. *Am. Stat.* **36**, 46–48 (1982).

291 25. Ballouz, S. & Gillis, J. AuPairWise: A method to estimate RNA-Seq replicability through co-expression. *PLoS Comput.
Biol.* **12**, e1004868 (2016).

293 26. Hart, T., Brown, K. R., Sircoulomb, F., Rottapel, R. & Moffat, J. Measuring error rates in genomic perturbation screens:
294 gold standards for human functional genomics. *Mol. Syst. Biol.* **10**, 733 (2014).

295 27. Vinceti, A., Perron, U., Trastulla, L. & Iorio, F. Reduced gene templates for supervised analysis of scale-limited
296 CRISPR-Cas9 fitness screens. *Cell Rep.* **40**, 111145 (2022).

297 28. Hart, T. & Moffat, J. BAGEL: a computational framework for identifying essential genes from pooled library screens.
298 *BMC Bioinforma.* **17**, 164 (2016).

299 29. Glass, G. V., McGaw, B. & Smith, M. L. *Meta-Analysis in Social Research* (SAGE Publications, 1981).

300 30. Yoshihama, M. *et al.* The human ribosomal protein genes: sequencing and comparative analysis of 73 genes. *Genome Res.*
301 **12**, 379–390 (2002).

302 31. Hart, T. & Moffat, J. BAGEL: a computational framework for identifying essential genes from pooled library screens.
303 *BMC Bioinforma.* **17**, 164 (2016).

304 32. Cohen, J. Statistical power analysis for the behavioral sciences. 1988, hillsdale, NJ: L. Lawrence Erlbaum Assoc. (1988).

305 Acknowledgements

306 IM was supported by fellowships from the INCIPIT PhD program co-funded by Horizon 2020-COFUND Marie Skłodowska-
307 Curie Actions, and an EMBO short-term fellowship (8536). This work has been partially funded by OpenTargets (OTAR-015
308 and OTAR2-055), and by Wellcome Trust Grant 206194. For the purpose of open access, the authors have applied a CC BY
309 public copyright licence to any Author Accepted Manuscript version arising from this submission.

310 Author contributions statement

311 RMI, FI, MJG conceived the study; RMI, IM, CP designed, and performed the benchmark analyses; RMI assembled the Jupyter
312 notebook; RMI, AS, IM, CP, FI wrote and revised the manuscript; FB performed experiments underlying the HT-29 reference
313 dataset under the supervision of MJG; RMI, IM, AS, interpreted results and assembled figures; MG and MJG contributed to
314 study supervision; AS and FI supervised the study. All authors read and revised the manuscript.

315 Competing interests

316 MJG has received research grants from AstraZeneca, GlaxoSmithKline, and Astex Pharmaceuticals, and is founder of Mosaic
317 Therapeutic. FI has received funding from Open Targets, a public-private initiative involving academia and industry, and he
318 performs consultancy for the joint CRUK-AstraZeneca Functional Genomics Centre and for Mosaic Therapeutics.

319 **Figures & Tables**

Sanger library version	Experiments identifiers	N. of replicates	Cas9 activity	Average transfection efficiency	Average Puromycin selection
1.0	HT29_c903	6	94.8%	2.33%	83.53%
1.0	HT29_c904	3	94.8%	27.57%	89.97%
1.1	HT29_c905	9	94.8%	33.42%	80.81%
1.1	HT29_c906	6	94.8%	35.65%	88.40%
1.1	HT29_c907	3	94.8%	32.40%	89.07%
1.1	HT29_c908	3	94.8%	32%	79.33%

Table 1. Reference HT-29 screening dataset. Libraries, experiment identifiers and transfection/selection efficiencies across screens.

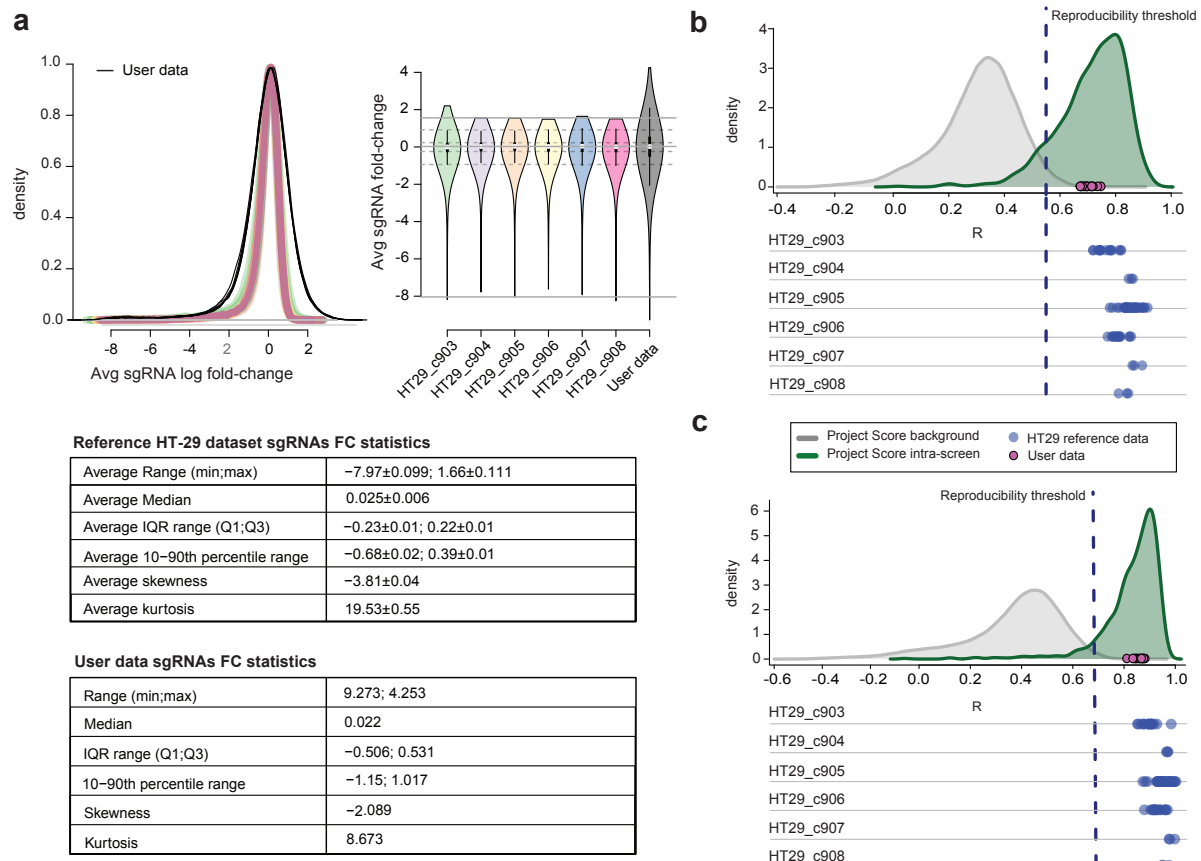


Figure 1. (a) Distributions of single-guide RNA (sgRNA) depletion log fold-changes and their average parameters (with confidence intervals) across the different screens of the reference HT-29 dataset, and in an example of user-provided screen performed using reagent and experimental settings described in Behan *et al.*⁷ and the Sanger library. (bc) Outcomes from an evaluation of inter-screen similarity. Distributions of pairwise Pearson’s correlation scores computed between gene essentiality profiles of replicates for each of the six HT-29 reference screens (blue dots), considering depletion log fold-changes of highly reproducible/informative sgRNAs only. Their value is abundantly larger than the quality control threshold defined from the analysis of the Project Score dataset (dark blue dashed vertical line), both at sgRNA- (b) and gene-level (c). The distribution of correlations from comparing replicates of the same screen in Project Score is shown in green, while the distribution of correlations from comparing each possible pair of replicates (regardless the screen) is shown in grey, with densities varying according to the level inspected (sgRNA or gene). The magenta points indicate correlation between pairs of replicates of an example user-provided screen of the HT-29 cell line (performed using the same setting of Behan *et al.*⁷) and the Sanger library¹⁶ which in this case exceeds the reproducibility threshold.¹⁶

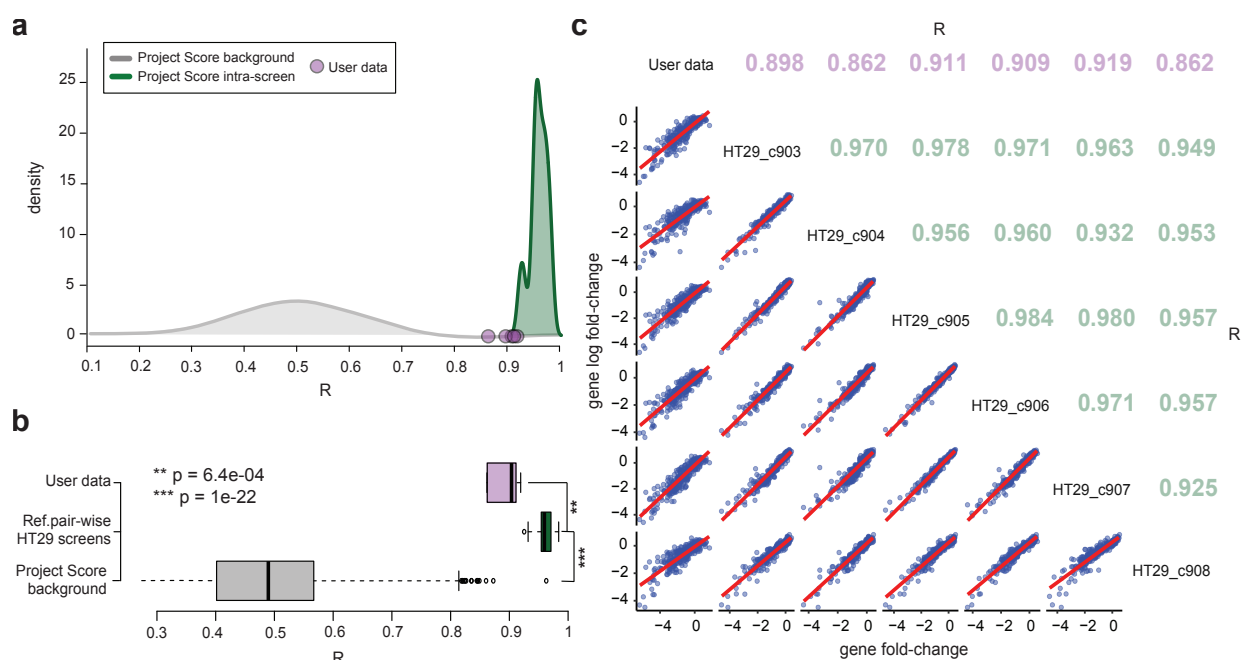


Figure 2. Inter-screen similarity evaluation. (a) Pearson's correlation scores between profiles of depletion log fold-changes (LFCs) computed at the gene level using the subset of reproducible and highly informative sgRNAs ($n = 838$) between pairs of HT-29 screens (in green) and between the HT-29 reference screens and an example user-provided screen (in pink), with replicates collapsed by LFC averaging. The distribution in grey are computed between each possible pair of screen replicates in Project Score, to estimate expectation is also visualised (in gray). (b) Two-sided t-test comparing expected Project Score correlation scores versus those computed between each pair of screens in the HT-29 reference dataset, as well as those computed between the example data screens versus those computed in the HT-29 reference dataset. The reference dataset scores are largely significantly different from expectation, the user data scores are still largely different from expectation but not as much as the reference data. (c) Scatter-plot correlation matrix showing pairwise Pearson's correlation scores computed within HT-29 references and between user data versus HT-29 reference screens.

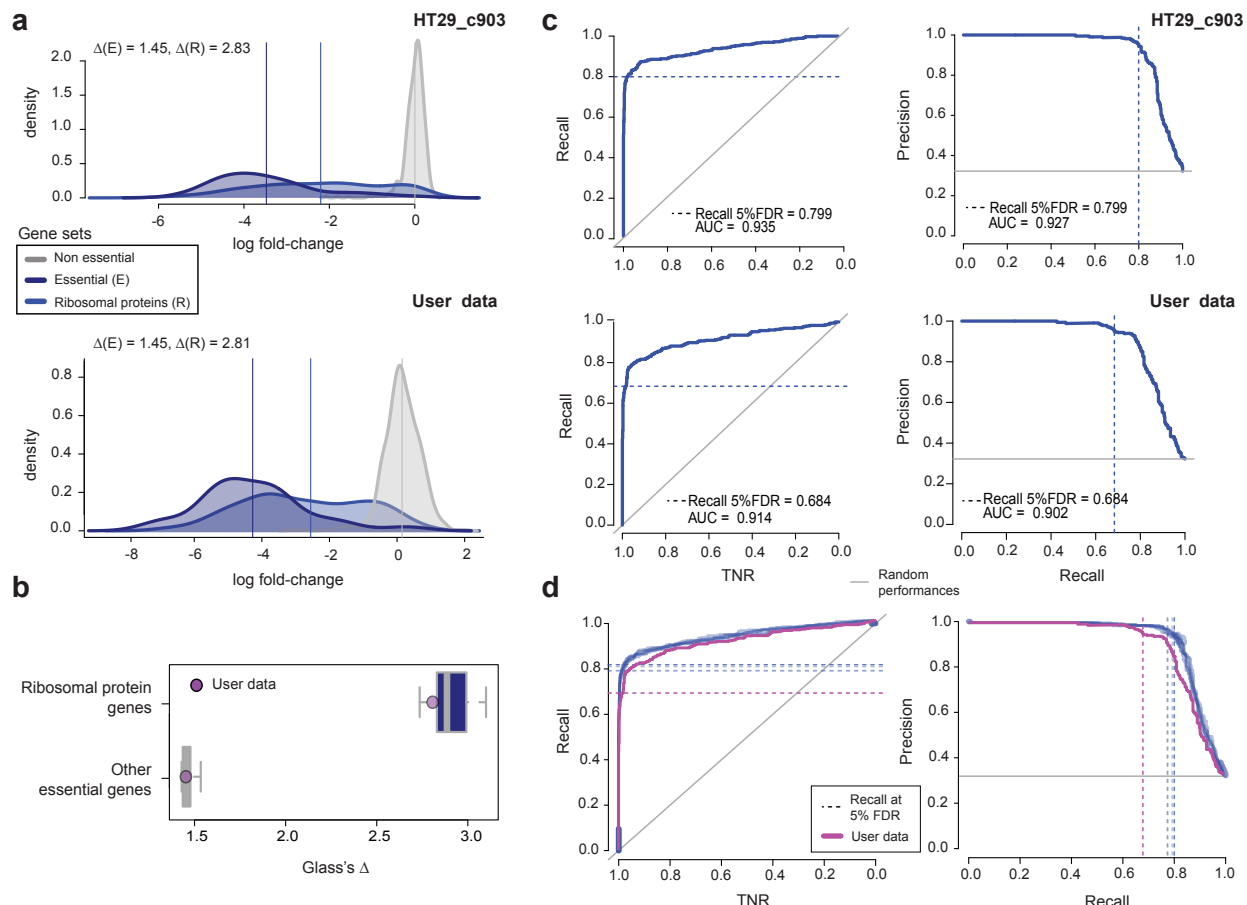


Figure 3. Screens' quality in terms of phenotype Intensity and receiver operating characteristic (ROC) analysis. (a) Distributions of gene depletion log fold-changes (LFCs) for one of the screens in the HT-29 reference dataset (at the top) and an example user-provided screen (at the bottom). Glass's Δ (GD) scores for reference essential genes (E) and ribosomal protein genes (R) with respect to non-essential genes are reported at the top of each plot. Vertical lines indicate mean LFCs for each gene set as indicated by the different colours. (b) Distributions of GD scores with respect to ribosomal protein genes and other essential genes (as indicated by the different colours), computed across the reference screens with overlaid GDs observed for the example user-provided screen. (c) ROC and Precision Recall (PrRc) curves quantifying the ability of a given screen in correctly classifying prior known essential and non-essential genes, based on their depletion LFCs for one of the screens in the HT-29 reference dataset (at the top) and an example user-provided screen (at the bottom). Recall of prior known essential genes at a 5% false discovery rate and areas under the curves are also reported, with the former indicated also by the dashed lines. (d) As for panel c but extended to all the reference screens and the user data, as indicated by the different colours.

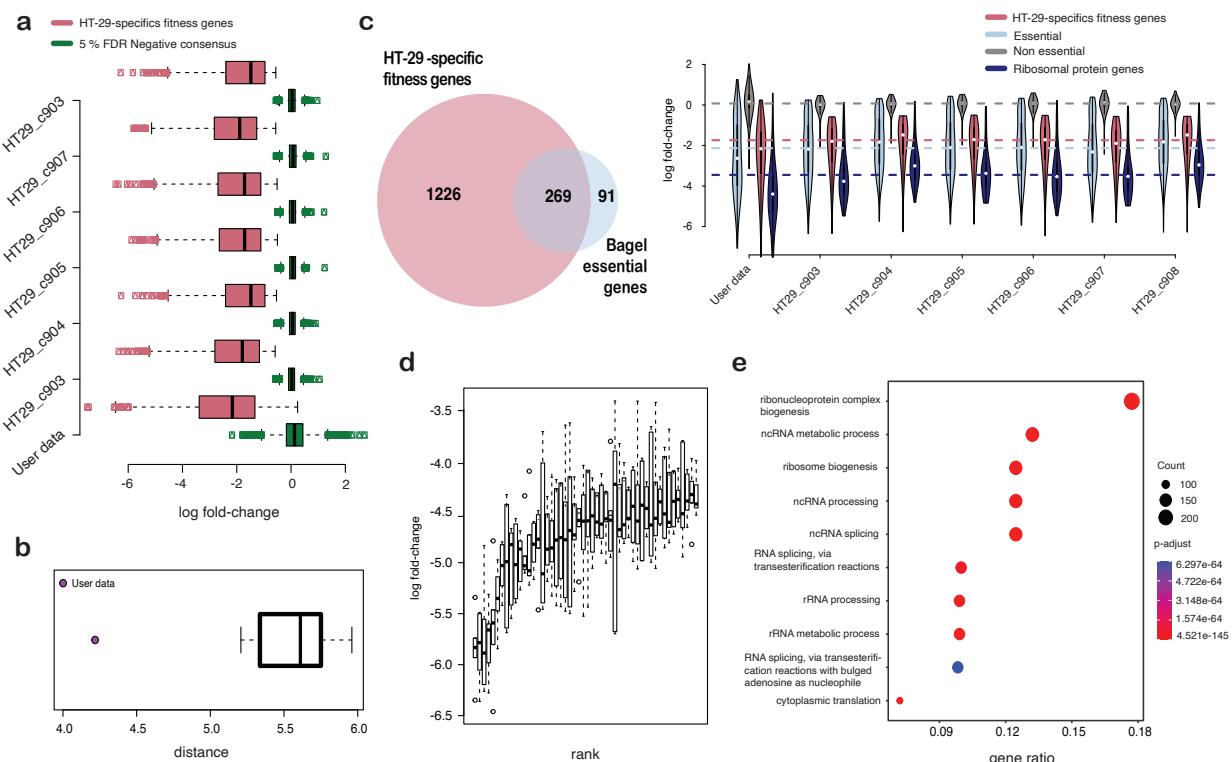


Figure 4. (a) Depletion log fold-change (LFCs) distributions of HT-29 specific positive and negative essential genes across individual reference HT-29 screens and example user-provided data. (b) Distribution of distances between HT-29 specific positive and negative essential genes, quantified through Cohen's d, across the reference HT-29 screens (the boxplot) or for the example user-provided data (which in this case does not meet expectations). (c) On the left, comparing the HT-29-specific essential genes and a widely used set of prior known essential genes highlights a statistically significant overlap (two-sided Fisher's exact test p-value = 7.1×10^{-221}); on the right, distribution of LFCs for different gene sets along with the HT-29-specific fitness genes across the reference HT-29 screens, as well as an example user-provided data. (d) Depletion LFCs of the top 50 HT-29-specific fitness genes consistently depleted in all experiments, across HT-29 reference screens. (e) Top 10 Gene Ontology categories (Biological ProcessP) significantly enriched (Benjamini-Hochberg corrected p-value < 0.05) in the HT-29-specific essential genes.